NMR spectroscopic investigation of benzothiazolylacetonitrile azo dyes: CR7 substitution effect and semiempirical study

H.M. Alsoghier [a,b,*], M. Abdellah [a,c,*], H.M. Rageh [a], H.M.A. Salman [a], M.A. Selim [a], M.A. Santos [b], S.A. Ibrahim [d]

[a] Chemistry Department, Faculty of Science, South Valley University, 83523 Qena, Egypt
[b] Centro de Química Estrutural, Instituto Superior Técnico, Universidade de Lisboa, Av. Rovisco Pais 1, 1049-001 Lisboa, Portugal
[c] Ångström Laboratory, Department of Chemistry, Uppsala University, Box 523, 75120 Uppsala, Sweden
[d] Chemistry Department, Faculty of Science, Assiut University, 71516 Assiut, Egypt

ARTICLE INFO

ABSTRACT

Ebead et al. had reported in the synthesis and the UV–Visible solvatochromism combined with semiempirical calculations to study the tautomerism of 1,3-benzothiazol-2-ylacetonitrile azo dyes [1]. In this study, 1,3-benzothiazol-2-ylacetonitrile azo dyes (1–6) have been resynthesized, one and two dimensional ^{1}H and ^{13}C NMR, as well as absorption and emission spectra, were collected and interpreted. The obtained results were used to clarify the tautomerization phenomenon of these dyes. Predominantly, these dyes exist in Z-hydrazone form reinforced through intramolecular hydrogen bonding in deuterated chloroform. Substituents (R) in carbon7 (CR7) are the key player of the changes in ^{1}H and ^{13}C NMR chemical shifts, also in the absorption and emission wavelengths of benzothiazole azo dyes. Also, the relative photoluminescence quantum yields (PL QY) of these dyes (1–6) were estimated and related to the nature of substituents. Finally, PM6 semiempirical calculations were employed to confirm the preferred geometric structure and experimental NMR, absorption, and emission results.

1. Introduction

Azo dyes are still a favourite destination for many fascinated people in current years [2–4]. Recently, benzothiazole azo dyes are the cornerstone in modern applications such as liquid crystal displays (LCDs) [5], nonlinear optical (NLO) apparatus [6–8], dye-sensitized solar cells (DSSCs) [9], optoelectronic devices [10], and in biological and medical studies [11]. These electronic applications are spawned from the tautomerism phenomenon and structural conversions of these dyes [5–10]. Depending on experimental UV–Visible spectra in different solvents and semiempirical PM6 calculations [1], 1,3-benzothiazol-2-ylacetonitrile azo dyes coexisted mainly in E-azo-enamine and E-hydrazone tautomeric forms. However, X-ray crystallographic data reveal that 1,3-benzothiazol-2-yl-(4-methylphenyl)diazenylacetonitrile (3p-CH₃) dye exists only in Z-hydrazone form [12] stabilized through intramolecular hydrogen bonding in the solid crystal [13]. Herein, we removed the structure ambiguity between Ebead et al. [1] and Badahdah [12,13] of these dyes by experimental investigation of the tautomeric phenomenon of benzothiazolylacetonitrile azo dyes in solution, and the role of one and two dimensional ^{1}H and ^{13}C NMR

in understanding this phenomenon as well as to prove the predominant conformational form in a nonpolar solvent. Moreover, the (CR7) substituents play a pivotal effect on the chemical shifts (δ) of protons and carbons, the semiempirical physicochemical parameters, also on the absorption and photoluminescence properties of our investigated dyes.

2. Experimental

2.1. Synthesis of 1,3-benzothiazol-2-ylacetonitrile azo dyes 1–6

Dyes (1–6) under investigation (Scheme 1) were synthesized according to the procedure described in the literature [1,12,14]. Briefly, to an ethanolic solution of 1,3-benzothiazole-2-ylacetonitrile (0.01 mol) in the presence of sodium acetate (≈ 0.01 mol) in an ice bath, a solution of diazotized aromatic amines was added drop wisely with vigorous stirring at 0–5 °C for one hour (for more details see the Supplementary material) (Scheme 1).
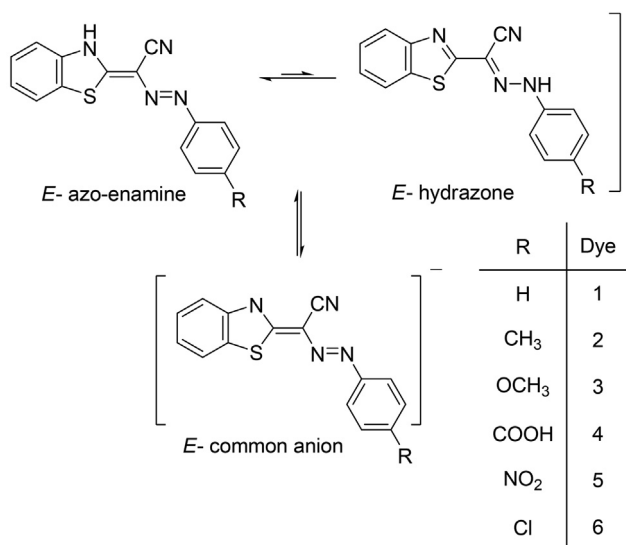
Scheme 1. The suggested equilibrium of dyes (**1–6**) from the point of view of *Y.H. Ebead et al.* [1].

2.2. NMR spectroscopy measurements

The ^{1}H and ^{13}C NMR spectra were recorded on Bruker AvanceII + 400 MHz, 9.4 T, Ultrashielded 1H frequency: 400 MHz spectrometers operating at 400.13 MHz for ^{1}H and 100.62 MHz for ^{13}C. The samples were dissolved in CDCl$_3$ but compound (**4p**-COOH) in (CD$_3$)$_2$SO because of sparing solubility in CDCl$_3$. The ^{1}H and ^{13}C chemical shifts (δ) are expressed in ppm referenced to the central peak of the solvents CDCl$_3$ (δ = 7.26 (^{1}H) and 77.16 (^{13}C)) and (CD$_3$)$_2$SO (δ = 2.50 (^{1}H) and 39.5 (^{13}C)). All 2D experiments (COSY, HMQC, and HMBC) were performed using the manufacturer's software (TOPSPIN 2.1). All the measurements were achieved at room temperature (≈ 25 °C).

2.3. UV–Visible spectroscopy measurements

Electronic UV–Visible absorption spectra were monitored by a Shimadzu 2401PC spectrophotometer (equipped with a Julabo F30 ultrathermostat with an accuracy of ± 0.5 °C) within the wavelength range 200–800 nm using thermostated (T = 25.0 ± 0.2 °C) 1 cm matched quartz cells. The dyes (**1–6**) were dissolved in CHCl$_3$ (99.0–99.4% BDH AnalaR), but the dye (**4p**-COOH) shows sparing solubility and so the undissolved dye was filtered off to get a clear chloroformed solution. The concentration of UV–Visible measured chloroformed solutions of dyes (**1–6**) was 1–2 × 10^{-5} M.

2.4. Fluorescence spectroscopy measurements

The fluorescence emission spectra of the same UV–Visible chloroformed solutions of dyes (**1–6**) were measured by JASCO Spectrofluorometer FP-8500 at different excitation wavelengths 400–423 nm; excitation and emission bandwidth are 5 nm, and scan rate is 1000 nm/min.

The relative photoluminescence quantum yield (PL QY) of the dyes was measured and estimated by comparing the dye's PL intensities with that of standard coumarin 102 dye at the same optical density (0.09) as:

$$\varnothing_{f,x} = \varnothing_{f,st} \cdot \frac{F_x}{F_{st}} \cdot \frac{f_{st}(\lambda_{ex})}{f_x(\lambda_{ex})} \cdot \frac{n_x^2}{n_{st}^2}$$

$$f_x(\lambda_{ex}) = 1 - 10^{-A(\lambda_{ex})}$$

where $\Phi_{f,x}$ is the quantum yield for the dye, $\Phi_{f,st}$ = 0.764 is the quantum yield for the standard dye (coumarin 102), F_{st} and F_x are the area under the emission spectrum of the standard dye and one of the under investigation azo dyes (**1–6**), respectively, and n_x = 1.50 and n_{st} = 1.44 are the refractive index for the used solvent namely, chloroform (for the dyes) and ethanol for coumarin 102 [15,16].

2.5. Quantum computational calculations

Structure optimization of the dyes (**1–6**) in the ground (S$_0$) and first excited (S$_1$) states were performed using the semiempirical PM6 and PM6/CI methods. The geometric structure of the *Z*-hydrazone form of these dyes was generated by replacing a methyl group in the single crystallographic structure of 1,3-Benzothiazol-2-yl((4-methylphenyl)hydrazono)acetonitrile dye (CDS Entry: COWGUR [13], Deposition Number: 617431) with other substituents (H, OCH$_3$, COOH, NO$_2$, Cl). Enthalpy of formation, dipole moments, and energies of natural molecular orbitals (HOMO&LUMO) of these azo dyes were isolated trustily from the PM6 and PM6/CI geometric optimized MOPAC data files. All geometry calculations were obtained from MOPAC 2009— free license on the internet and done on a Personal laptop computer.

3. Results and discussion

Azo-hydrazone tautomerization is a well-recognized phenomenon in azo dyes, but still not yet completely clear [17–19]. Nuclear magnetic resonance (NMR) spectroscopy in one and two dimensions is a powerful tool for the characterization and examination of azo-hydrazone tautomerism in solutions of azo dyes [19–23].

3.1. One and two dimensional ^{1}H and ^{13}C NMR for investigation of tautomerism of dyes (1–6)

According to semiempirical PM6 calculations and UV–Visible spectra in different solvents [1], benzothiazolylacetonitrile azo dyes coexisted geometrically in *E* configuration as azo-enamine and/or hydrazone-common anion equilibrium as shown in Scheme 1 [1].

However, one and two-dimensional ^{1}H and ^{13}C NMR studies of dyes (**1, 2, 3, 5, 6**) in CDCl$_3$ solution reveal that these dyes commonly exist in *Z* geometric configuration as hydrazone form (Scheme 2).

This fact is the result of the presence of an intramolecular hydrogen bond between hydrazone (**H-N1**) proton and the nitrogen atom (**N**) in benzothiazole ring [12,13]. Furthermore, the intramolecular hydrogen bond is the main reason for high downfield chemical shift (δ = 14.31–14.53 ppm) of hydrazone (**H-N1**) proton comparing to (**H-N1**) proton (δ = 12.40 ppm) in dye (**4p**-COOH) (see Fig. 1 and Table 1) [19,20,24,25].

For investigation and examination of the geometric chemical structure and tautomerism of dyes (**1–6**), we applied two-dimensional COSY, HMQC, and HMBC experiments [20,26] for assignment of the ^{1}H chemical shifts, protonated carbons, and quaternary carbons, respectively, as well as discovering the most favourable tautomeric form in solutions (Table 1).

The HMBC spectra of dyes (**1, 2, 3, 6**) revealed a correlation of the hydrazone (**H-N1**) proton (δ = 14.31–14.37 ppm) with the **o-C3,4** carbons (δ = 115.72–117.12 ppm), the **C2** carbon (δ = 135.42–141.75 ppm) in the benzene ring and the **9′C = N** carbon (δ = 106.02–107.74 ppm) (Fig. 2, Table 1). But for dye (**5p**-NO$_2$), the hydrazone (**H-N1**) proton correlation with the **o-C3,4** carbon, the **C2** carbon, and **9′C = N** carbon is not so clear, which may be due to the partial solubility of compound (**5p**-NO$_2$) in CDCl$_3$. The HMBC results proved indubitably that the predominant conformational structure of these dyes is *Z*-hydrazone form accompanied by an intramolecular hydrogen bond between the hydrazone (**H-N1**) proton and the nitrogen atom (**N**) in benzothiazole ring [12,13].
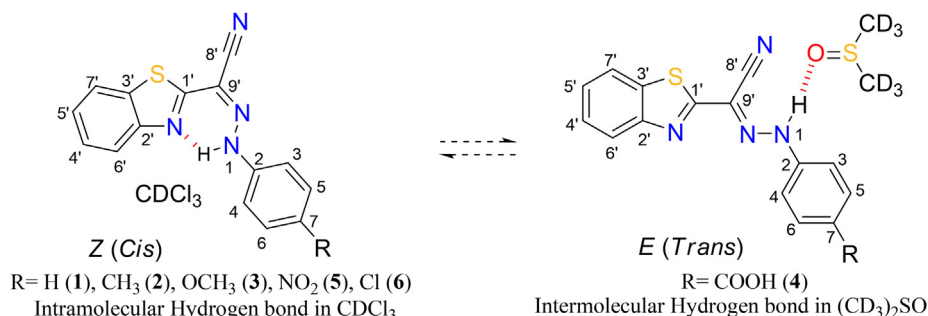
Scheme 2. The intra and intermolecular hydrogen bonds of the predominant *Z*- and *E*- hydrazone forms of dyes (1,2,3,5,6) and (4), respectively. (*Numbering of carbons and protons will not be continuous and not follow numbering rules, where the benzothiazolylacetonitrile moiety has numbers from 1′ to 9′, on the other hand, the substituted phenyl ring has numbers from 1 to 7.
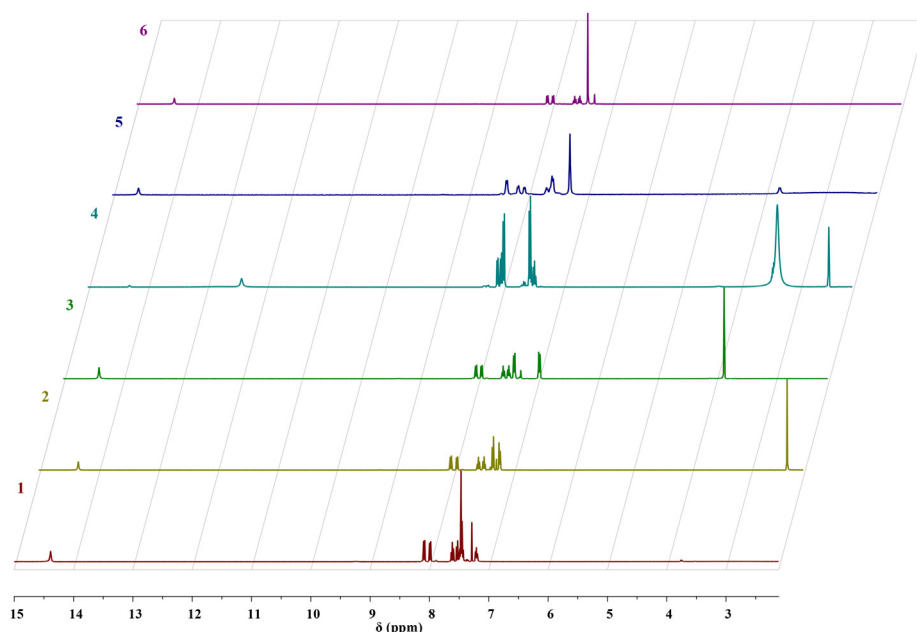

Fig. 1. Normalized ^{1}H NMR spectra of azo dyes (**1,2,3,5,6**) in CDCl$_3$ and (**4**) in (CD$_3$)$_2$SO.

However, in deuterated DMSO, dye (**4***p*-COOH) shows an upfield chemical shift (δ = 12.40 ppm) of hydrazone (**H-N1**) proton comparing to other dyes (**1,2,3,5,6**) in CDCl$_3$ (Fig. 1 and Table 1). This shift may be attributed to the presence of an intermolecular hydrogen bond between the hydrazone (**H-N1**) proton and the solvent (CD$_3$)$_2$SO (Scheme 2) [24,27–29].

3.2. Substituents (CR7) effect on the chemical shifts (δ) of ^{1}H and ^{13}C NMR of dyes (1–6)

Our investigated dyes (**1–6**) show different chemical shifts (δ) of both ^{1}H and ^{13}C depending essentially on the substituted groups (**R**) in carbon **C7** in benzene ring (**CR7** effect). The electron-donating or withdrawing nature of the **CR7** substituent groups is the key player in the chemical shifts (δ) positions of protons and carbons.

Generally, proton and carbon chemical shifts (δ) are much more affected by the nature of **CR7** substituent groups in the benzene ring than in the benzothiazole ring [19,30], although the proton chemical shifts (δ) are much more affected than those of the carbons (Table 1).

The presence of electron-donating **CR7** substituents in compounds (**2***p*-CH$_3$) and (**3***p*-OCH$_3$) results in the chemical shift of protons and most carbons moving upfield as compared to the dye (**1***p*-H). High electron donation of these substituent groups caused a high shielding

effect on most positions especially in *ortho* and *para* carbons **C5,6** and **C2** in the benzene ring, where **C2** carbon in dyes (**2***p*-CH$_3$) and (**3***p*-OCH$_3$) shifts to upfield by 2.32 and 6.33 ppm, respectively comparing to dye (**1***p*-H) as shown in Table 1. These findings result from the fact that the OCH$_3$ group has higher electron donation ability than the CH$_3$ group, namely due to the extra resonance donation, and the electron density moves from electron-donating substituted benzene ring to benzothiazole ring.

However, the insertion of an electron-withdrawing group (NO$_2$) in carbon **C7** of dye (**5***p*-NO$_2$) shows downfield chemical shifts of protons and most carbons as compared with the non-substituted dye (**1***p*-H). Furthermore, the anisotropic deshielding effect [19,30,31] of the nitro group pushes the chemical shift of protons of the adjacent carbons **C5,6** to higher downfield (ca 0.78 ppm) as compared with those of carbons **C3,4** (Table 1). Similar behaviour is observed for the carboxylic group in the compound (**4***p*-COOH), despite changing of deuterated solvents, and these results indicate that electron-withdrawing substituent groups (**CR7**) reverse the electron density movement toward the benzene ring. For dye (**6***p*-Cl), the lower resonance donation with the inductive withdrawal electronic effect of the chloro-substituent group (Cl) [19,30,31] causes no significant chemical shifts of protons and carbons comparing to dye (**1***p*-H).

Table 1

^{1}H and ^{13}C chemical shifts (ppm) and protons coupling constants (J) of dyes (**1, 2, 3, 5, 6**) in CDCl$_3$, but dye (**4**) in DMSO d_6.

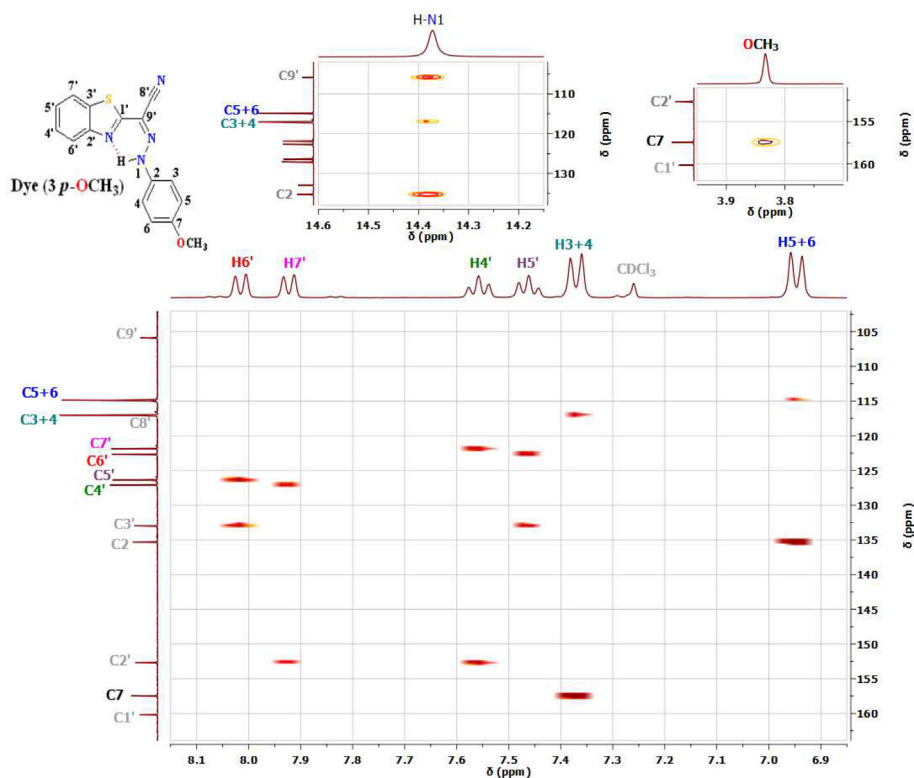| H/C No.	1 (*p*-H)		2 (*p*-CH$_3$)		3 (*p*-OCH$_3$)		4 (*p*-COOH)		5 (*p*-NO$_2$)		6(*p*-Cl)	
	δ(^{1}H)	δ(^{13}C)	δ(^{1}H)	δ(^{13}C)	δ(^{1}H)	δ(^{13}C)	δ(^{1}H)	δ(^{13}C)	δ(^{1}H)	δ(^{13}C)	δ(^{1}H)	δ(^{13}C)
1′	–	160.1	–	160.14	–	160.28	–	163.8	–	159.44	–	159.93
2′	–	152.8	–	152.76	–	152.76	–	152.93	–	152.67	–	152.68
3′	–	133.27	–	133.14	–	133.09	–	133.78	–	133.66	–	133.28
4′	7.61–7.57 (m, 1H)	127.35	7.59–7.54 (m, 1H)	127.25	7.56 (t, J = 7.7 Hz, 1H)	127.21	7.54–7.51 (m, 1H)	126.78	7.68–7.63 (m, 1H)	127.87	7.59 (t, J = 7.6 Hz, 1H)	127.46
5′	7.52–7.48 (m, 1H)	126.76	7.49–7.45 (m, 1H)	126.59	7.46 (t, J = 7.5 Hz, 1H)	126.5	7.49–7.43 (m, 1H)	126.1	7.60–7.57 (m, 1H)	127.56	7.51 (t, J = 7.5 Hz, 1H)	126.92
6′	8.06 (d, J = 8.2 Hz, 1H)	123.03	8.03 (d, J=8.2 Hz, 1H)	122.9	8.02 (d, J = 8.1 Hz, 1H)	122.79	8.03 (d, J = 7.6 Hz, 1H)	122.96	8.13 (d, J = 8.0 Hz, 1H)	123.5	8.06 (d, J = 8.2 Hz, 1H)	123.08
7′	7.96 (d, J = 8.0 Hz, 1H)	122.07	7.93 (d, J=8.0 Hz, 1H)	121.97	7.92 (d, J = 8.0 Hz, 1H)	121.97	8.09 (d, J = 7.3 Hz, 1H)	122.22	8.03 (d, J = 7.7 Hz, 1H)	122.31	7.96 (d, J = 8.0 Hz, 1H)	122.1
8′	–	116.87	–	117.03	–	117.19	–	110.4	–	115.81	–	116.58
9′	–	107.2	–	106.49	–	106.02	–	110.21	–	110.82	–	107.74
2	–	141.75	–	139.43	–	135.42	–	145.79	–	146.77	–	140.35
3,4	7.44 (d, J = 1.6 Hz, 2H)	115.83	7.32 (d, J=8.4 Hz, 2H)	115.72	7.37 (d, J = 8.7 Hz, 2H)	117.12	7.54 (d, J = 8.8 Hz, 2H)	114.97	7.55 (d, J = 7.9 Hz, 2H)	115.49	7.37 (s, 4H)	116.9
5,6	7.44–7.40 (m, 2H)	129.76	7.21 (d, J=8.3 Hz, 2H)	130.26	6.95 (d, J = 8.7 Hz, 2H)	115	7.98 (d, J = 8.8 Hz, 2H)	131.05	8.33 (d, J = 8.4 Hz, 2H)	126.02		129.82
7	7.18 (tt, J = 6.7, 1.8 Hz, 1H)	125.33	–	135.22	–	157.58	–	125.78	–	144.33	–	130.36
1N-H hydrazone	14.36 (s, 1H)	–	14.31 (s, 1H)	–	14.37 (s, 1H)	–	12.40 (s, 1H)	–	14.53 (s, 1H)	–	14.34 (s, 1H)	–
p-CH$_3$			2.36 (s, 3H)	21.1								
p-OCH$_3$					3.83 (s, 3H)	55.73						
p-COOH							12.80 (b, 1H)	166.87				

Fig. 2. HMBC spectrum of azo dye (**3**) in CDCl₃; HMBC spectrum of hydrazone (**H-N1**) and (OCH₃) protons of this dye in CDCl₃ (inserted).

According to the ¹H and ¹³C NMR study of dyes (**1**–**3**, **5**, **6**) in CDCl₃, we discover that the predominant tautomeric structure of these dyes is *Z*-hydrazone form. Besides the main protons and carbons resonance peaks of investigated dyes (Table 1), we observe accompanied tiny peaks near carbons **C2**, **C3,4**, **C5,6**, and **C7** of the substituted benzene ring. These accompanied tiny peaks may be attributed to the disappearance of the symmetry plane of the substituted benzene ring because of the ability of CDCl₃ to interact with investigated dyes via intermolecular hydrogen bond or dipole–dipole interaction [32]. The ratio between the integration of the accompanied tiny peaks to the
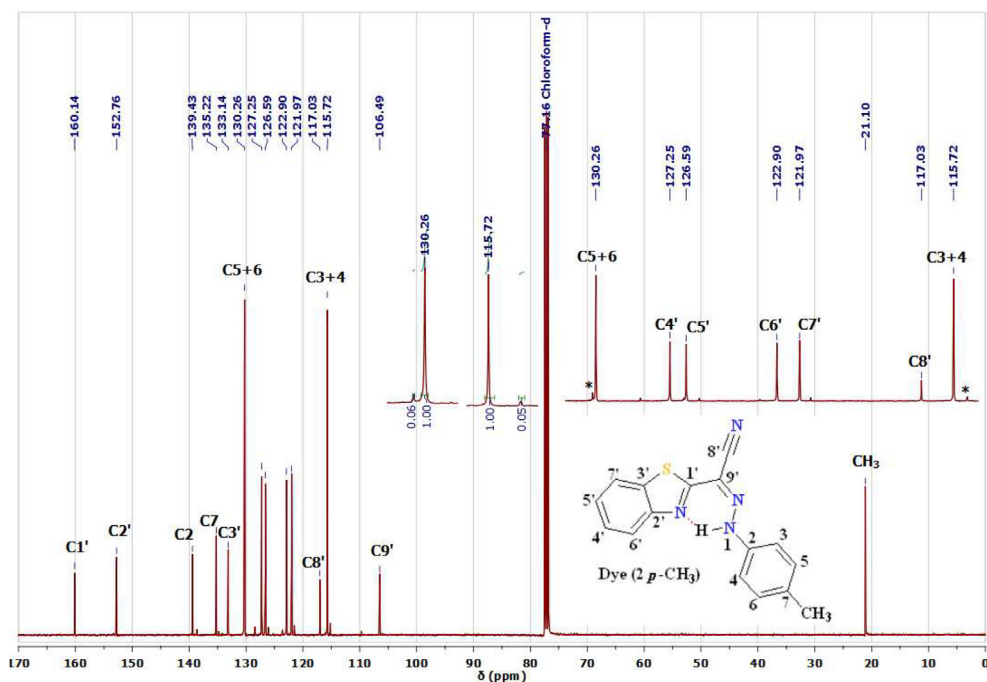

Fig. 3. ¹³C NMR spectra of azo dyes (**2**) in CDCl₃, expansion of integrated C3,4 and C5,6 (inserted) and *noted for accompanied tiny peaks.

Table 2

Experimental electronic absorption, emission, and optical energy gap data of dyes (**1**–**6**) in CHCl$_3$ and PM6 theoretical energy difference ($\Delta E_{S1\text{-}S0}$) between excited(S$_1$) and ground (S$_0$) states.

Dyes	Absorption		Emission		$\Delta\lambda_{St}$ (nm)	QY %	E$_g$ (eV)	$\Delta E_{S1\text{-}S0}$ (eV)
	λ_{max} (nm)	log ε	λ_{ex} (nm)	λ_{em} (nm)				
1 (*p*-H)	403.50	4.57	400.00	483.50	80.00	0.05	3.07	2.976
2 (*p*-CH$_3$)	411.00	4.58	411.00	509.50	98.50	0.09	3.01	2.933
3 (*p*-OCH$_3$)	423.00	4.60	423.00	528.00	105.00	0.08	2.93	2.899
4 (*p*-COOH)	405.50	N. D.	405.00	478.50	73.00	0.06	3.05	3.006
5 (*p*-NO$_2$)	408.50	4.75	408.00	471.50	63.00	0.074	3.03	3.001
6 (*p*-Cl)	405.00	4.55	400.00	501.00	96.00	0.062	3.06	2.959

$\Delta\lambda_{St}$ is the Stokes' shift ($\lambda_{em} - \lambda_{max}$) and N. D. is not determined.

main peaks of carbons **C3,4** and **C5,6** is 5–6% for dyes (**1**–**3**, **6**), but for dye (**5***p*-NO$_2$) is 9–10% (Fig. 3). This result suggests that in CDCl$_3$ at least 90% of these dyes exist predominantly as *Z*-hydrazone form stabilized by an intramolecular hydrogen bond. Conversely, preliminary NMR studies in DMSO indicate a probable existence of the *E*-hydrazone form stabilized by intermolecular H-bonding interaction with the solvent, beside the *Z*-hydrazone form.

3.3. Substituents (CR7) effect on the absorption and emission spectra of dyes (1–6) in chloroform

Besides NMR, electronic absorption and emission spectra are common tools for discovering tautomerism of azo dyes [1,22,33–37]. In chloroform, **CR7** substituent groups are the principal player for shifting the values of maximum λ_{max} and emission λ_{em} wavelengths of the main single absorption and emission bands as shown in Table 2.

Absorption spectra of investigated dyes represent in Fig. 4, The main single absorption bands at longer wavelengths (403–423 nm) are assigned to π-π* transition in *Z*-hydrazone form accompanied by intramolecular charge transfer (CT) nature [1,12].

λ_{max} of the main absorption band depends mainly on the substituted **R** groups attached to **C7** in phenyl ring, electron-donating methoxy (OCH$_3$) and methyl (CH$_3$) groups shift the λ_{max} to redder wavelength than electron-withdrawing groups (COOH and NO$_2$) (Table 2). This shift can be attributed to the electron pushing-ability of donor groups towards the conjugated π system in investigated dyes comparing to acceptor groups [1,18,19,35].

For dye (**5***p*-NO$_2$) the main absorption band is accompanied by a shoulder at a longer wavelength (424 nm), which should be attributed to the appearance of *E*-hydrazone form besides the still predominant *Z*-hydrazone form. The intensity of the shoulder increased with dilution,

giving support to the existence of intermolecular interaction between the dye and chloroform [32], which may be responsible for the shifting of the dominant *Z*-hydrazone form to *E*-hydrazone form inconsistency with NMR results.

Normalized emission spectra of investigated dyes (Fig. 5) showed that in dyes with electron-donating groups, (**2***p*-CH$_3$) and (**3***p*-OCH$_3$), the emission wavelength, λ_{em}, is redshifted, whereas those with electron-withdrawing groups, (**4***p*-COOH) and (**5***p*-NO$_2$), emit light at a shorter wavelength, comparing to dye (**1***p*-H) (Table 2).

This fluorescence results shed more light on electron pushing-ability of donor groups towards the conjugated π system and decreasing the HOMO–LUMO bandgap in dyes (**2***p*-CH$_3$) and (**3***p*-OCH$_3$), while electron acceptor groups in dyes (**4***p*-COOH) and (**5***p*-NO$_2$) showing opposite effect [38–40]. Moreover, the relative photoluminescence quantum yield (PL QY) of these dyes was measured and estimated by comparing the dye's PL intensities with that of standard coumarin 102 dye at the same optical density as shown in Table 2. These benzothiazolylacetonitrile azo dyes have low photoluminescence quantum yields consistent with the aforementioned studies of azo dyes [16,41,42]. Also, dyes with electron donor groups (**2***p*-CH$_3$) and (**3***p*-OCH$_3$) show a tendency to give higher fluorescence quantum yield (PL QY) comparing to dyes with electron acceptor groups (**4***p*-COOH) and (**5***p*-NO$_2$) (Table 2), this fact is due to a substantial quenching ability of electron-withdrawing groups [2,43].

3.4. Substituents (CR7) effect on the structure and semiempirical parameters of dyes (1–6)

Semiempirical calculations are an aiding method for the investigation of tautomerism of azo dyes [1,22,44]. Our PM6 semiempirical
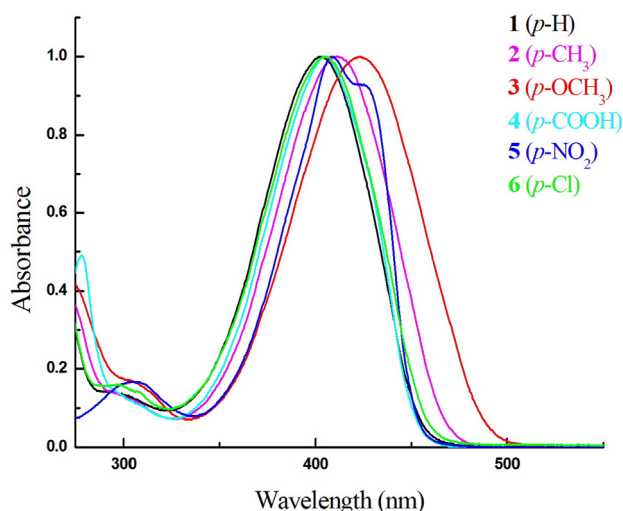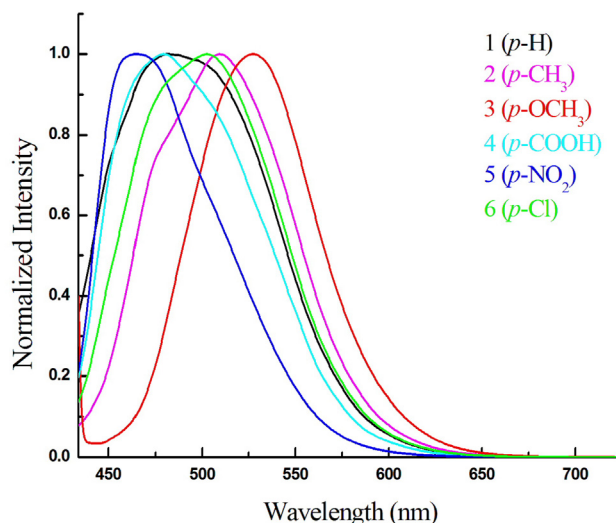

Fig. 4. Normalized absorption spectra of azo dyes (**1**–**6**) in CDCl$_3$.

Fig. 5. Normalized emission spectra of azo dyes (**1**–**6**) in CDCl$_3$.
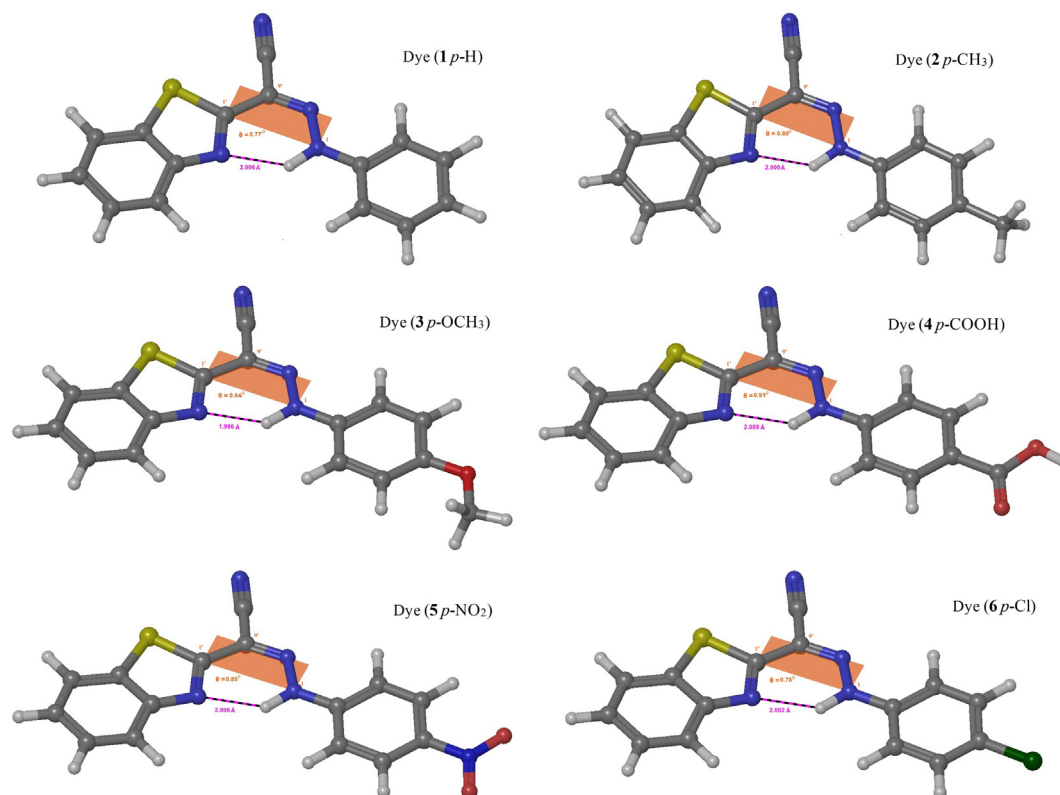
Fig. 6. Minimized Geometric models of azo dyes (**1–6**); Dashed Pink Line represents intramolecular hydrogen bond between hydrazone (**H-N1**) proton and the nitrogen atom (**N**) in benzothiazole ring, while Orange Plane represents the dihedral angle (Θ) between C1'-C9' = N-N1. (For interpretation of the references to colour in this figure legend, the reader is referred to the web version of this article.)

Table 3
PM6 (S_0 state) and PM6/CI (S_1 state) physicochemical parameters predicted in the gaseous phase of *Z*-hydrazone and *E*-azo-enamine [1] forms of these azo dyes (**1–6**).

Dye	Form	$\Delta_{f,298}H°$ (kcal/mol)		ΔE_{S1-S0}	μ	μ_{S1}	μ_{S1}-μ	Energy (eV)		E_{LUMO} -E_{HOMO}
		S_0	S_1	(kcal/mol)	(D)	(D)	(D)	HOMO	LUMO	(eV)
1 (*p*-H)	*E*-azo-enamine[1]	144.84	204.2	59.36	7.5	5.61	−1.89	−8.48	−1.4	7.08
	Z-hydrazone	141.32	210.54	69.22	5.45	6	0.55	−8.82	−1.48	7.34
2 (*p*-CH₃)	*E*-azo-enamine[1]	134.36	194.64	60.28	7.5	6.08	−1.42	−8.34	−1.32	7.02
	Z-hydrazone	131.5	199.72	68.22	5.93	7.18	1.25	−8.66	−1.4	7.26
3 (*p*-OCH₃)	*E*-azo-enamine[1]	103.22	163.47	60.25	5.89	4.9	−0.99	−8.26	−1.28	6.98
	Z-hydrazone	101.2	168.62	67.42	4.97	7.03	2.06	−8.49	−1.37	7.12
4 (*p*-COOH)	*E*-azo-enamine[1]	56.47	113.88	57.41	7.55	5.89	−1.66	−8.74	−1.77	6.97
	Z-hydrazone	52.76	122.69	69.93	4.42	4.62	0.2	−9.17	−1.83	7.34
5 (*p*-NO₂)	*E*-azo-enamine[1]	139.23	201.61	62.38	11.16	8.98	−2.18	−9.03	−1.81	7.22
	Z-hydrazone	136.5	206.29	69.79	7.8	9.35	1.55	−9.39	−2.1	7.29
6 (*p*-Cl)	*E*-azo-enamine[1]	134.83	193.13	58.3	7.88	5.4	−2.48	−8.58	−1.56	7.02
	Z-hydrazone	132.11	200.93	68.82	5.17	5.16	−0.01	−8.9	−1.63	7.27

$\Delta_{f,298} H^o$– enthalpy of formation in the S_0 and S_1 states, μ, μ_{S1} – dipole moments (Debye) in the S_0 and the Franck-Condon S_1 states respectively; HOMO and LUMO in eV, indicate the energies of the highest occupied and lowest unoccupied molecular orbitals.

study of azo dyes (**1–6**) in gaseous ground state confirms the predominant existence of these dyes (**1–6**) in *Z*-hydrazone form [8,12,13] stabilized by an intramolecular hydrogen bond (Fig. 6). Minimized geometric structures of these dyes (**1–6**) in Fig. 6 reflect the planar structure of *Z*-hydrazone form (dihedral angles between C1'-C9' = N-N1 Θ = 0.64⁰ to 0.91⁰). Also, the occurrence of strong intramolecular hydrogen bond between hydrazone hydrogen (**H-N1**) atom and the benzothiazole nitrogen atom (**d** = 1.996 to 2.009 Å) as shown in Fig. 6 is the mainspring for high downfield chemical shift (δ = 14.31–14.53 ppm) of this hydrazone (**H-N1**) proton in NMR results [19,20]. The aforementioned results are in consistence with single crystallographic structure of 1,3-benzothiazol-2-yl((4-methylphenyl)hydrazono)acetonitrile azo dye (Θ = 1.8⁰, **d** = 1.9 Å) [12,13]. However, the nature of substituents (**CR7**) groups slightly affects the planar structure and the hydrogen bond intensity of *Z*-hydrazone form of these dyes (**1–6**). Whereas, insertion of electron donor groups in dyes (**2***p*-CH₃ (Θ = **0.80⁰** and **d** = **2.000** Å)) and (**3***p*-OCH₃ (Θ = **0.64⁰** and **d** = **1.996** Å)) shifts the geometric structure and hydrogen bond intensity of *Z*-hydrazone form to be more planar and stronger, respectively than electron acceptor groups in dyes (**4***p*-COOH (Θ = **0.91⁰** and **d** = **2.009** Å)) and (**5***p*-NO₂ (Θ = **0.85⁰** and **d** = **2.006** Å)) according to Fig. 6.

Furthermore, the PM6 ground gaseous state heat of formations calculations reveal that *Z*-hydrazone form is more energetic favourable for all dyes (**1–6**) by (−2.02 to −3.7 kcal/mol) than the next stable *E*-azo-enamine form [1] (Table 3). Also, the lower dipole moment

(μ) values in the ground state of *Z*-hydrazone form comparing to the higher values in the *E*-azo-enamine form [1], implies that the favourability of *Z*-hydrazone form in non-polar solvents (CHCl$_3$ solution) and the positions of the main absorption bands of the revealed tautomers should depend closely on the solvent polarity. As well as, experimental optical band gaps (E$_g$) and PM6 theoretical energy differences (ΔE$_{S1-S0}$) between excited (S$_1$) and ground (S$_0$) states of *Z*-hydrazone form were evaluated (Table 2). The experimental optical band gap (E$_g$ = 1240/λ$_{max}$) [45] values of the dyes (**1–6**) go hand in hand with PM6 theoretical energy differences (ΔE$_{S1-S0}$) of *Z*-hydrazone form as shown in Table 2, thus confirmed that the absorption bands at different maximum wavelengths (λ$_{max}$) are initiated from π-π* intramolecular charge transfer (ICT) S$_0$ → S$_1$ transition [45,46]. Moreover, the Absorption and fluorescence results are inconsistence with PM6 HOMO-LUMO molecular orbitals calculations of *Z*-hydrazone form, where electron pushing-ability of donor groups towards the conjugated π system decreases the LUMO-HOMO energy gap in dyes (**2***p*-CH$_3$ (7.26 eV)) and (**3***p*-OCH$_3$ (7.12 eV)), while electron acceptor groups in dyes (**4***p*-COOH (7.34 eV)) and (**5***p*-NO$_2$ (7.29 eV)) showing opposite effect [38–40] as represented in Table 3.

4. Conclusion

The study of dyes, using NMR, UV–Visible, and fluorescence spectroscopic techniques, reveals that the *Z*-hydrazone form is the predominant structure of these dyes in CDCl$_3$, the intramolecular hydrogen bond being the main reason for stabilization of *Z* structure and these results are in agreement with X-ray crystallographic data [12,13]. Substituent groups attached to carbon **C7** play the main role in the NMR chemical shifts (δ) of protons and carbons as well as in absorption and emission spectral properties, what is herein called the **CR7** effect. Also, the photoluminescence quantum yield (PL QY) and PM6 semiempirical calculations of these dyes were performed.

A preliminary NMR study of one compound (**4***p*-COOH) in DMSO *d$_6$* suggests a probable equilibrium between *Z* and *E* conformation in this polar solvent, but an NMR study of the tautomerism of these dyes in DMSO *d$_6$* comparing to NMR in CDCl$_3$ is under investigation, as well as the complexing ability of some of these dyes with transition metals.

Declaration of Competing Interest

The authors declare that they have no known competing financial interests or personal relationships that could have appeared to influence the work reported in this paper.

Acknowledgment

Appendix A. Supplementary data

Supplementary data to this article can be found online at https://doi.org/10.1016/j.rechem.2020.100088.

References

[1] Y.H. Ebead, M.A. Selim, S.A. Ibrahim, Solvatochromic, acid–base features and time effect of some azo dyes derived from 1,3-benzothiazol-2-ylacetonitrile: Experimental and semiempirical investigations, Spectrochim. Acta Part A Mol. Biomol. Spectrosc. 75 (2) (2010) 760–768, https://doi.org/10.1016/j.saa.2009.11.051.

[2] S.J. Porobić, B.Đ. Božić, M.D. Dramićanin, V. Vitnik, Ž. Vitnik, M. Marinović-Cincović, D.Ž. Mijin, Absorption and fluorescence spectral properties of azo dyes based on 3-amido-6-hydroxy-4-methyl-2-pyridone: Solvent and substituent effects, Dyes Pigm. 175 (2020) 108139, https://doi.org/10.1016/j.dyepig.2019.108139.

[3] M.R. Maliyappa, J. Keshavayya, M. Mahanthappa, Y. Shivaraj, K.V. Basavarajappa, 6-Substituted benzothiazole based dispersed azo dyes having pyrazole moiety: Synthesis, characterization, electrochemical and DFT studies, J. Mol. Struct. 1199 (2020) 126959.

[4] A.B. Fradj, A. Boubakri, A. Hafiane, S.B. Hamouda, Removal of azoic dyes from aqueous solutions by chitosan enhanced ultrafiltration, Results Chem. 2 (2020) 100017.

[5] X. Tong, Y. Zhao, Multiple photochemical processes in liquid crystalline azo dye-doped liquid crystals, Chem. Mater. 21 (2009) 4047–4054.

[6] M.M.M. Raposo, M.C.R. Castro, A.M.C. Fonseca, P. Schellenberg, M. Belsley, Design, synthesis, and characterization of the electrochemical, nonlinear optical properties, and theoretical studies of novel thienylpyrrole azo dyes bearing benzothiazole acceptor groups, Tetrahedron 67 (2011) 5189–5198.

[7] P.J. Coelho, M.C.R. Castro, A.M.C. Fonseca, M.M.M. Raposo, Photoswitching in azo dyes bearing thienylpyrrole and benzothiazole heterocyclic systems, Dyes Pigm. 92 (2012) 745–748.

[8] H.M. Alsoghier, M.A. Selim, H.M.A. Salman, H.M. Rageh, M.A. Santos, S.A. Ibrahim, M. Dongol, T. Soga, A.A. Abuelwafa, NMR spectroscopic, linear and non-linear optical properties of 1,3-benzothiazol-2-yl-(phenylhydrazono)acetonitrile (BTPA) azo dye, J. Mol. Struct. 1179 (2019) 315–324.

[9] S. Bagheri Novir, S.M. Hashemianzadeh, Density functional theory study of new azo dyes with different π-spacers for dye-sensitized solar cells, Spectrochim. Acta Part A Mol. Biomol. Spectrosc. 143 (2015) 20–34, https://doi.org/10.1016/j.saa.2015.02.026.

[10] R.V. Solomon, R. Jagadeesan, S.A. Vedha, P. Venuvanalingam, A DFT/TDDFT modelling of bithiophene azo chromophores for optoelectronic applications, Dyes Pigm. 100 (2014) 261–268.

[11] M.A. Gouda, H.F. Eldien, M.M. Girges, M.A. Berghot, Synthesis and antitumor evaluation of thiophene based azo dyes incorporating pyrazolone moiety, J. Saudi Chem. Soc. (2012).

[12] K.O. Badahdah, Arylhydrazononitriles as building blocks in heterocyclic synthesis: Synthesis of new benzothiazolyl-1,2,3-triazole amines and-1,2,3-triazol-4-yl-1,3,4-thiadiazole-5-ylamines, Heterocycles 75 (2008) 1623–1630.

[13] K.O. Badahdah, CCDC 617431: Experimental Crystal Structure Determination, (2009).

[14] S. Rida, F. Ashour, S. Elhawash, M. Elsemary, M. Badr, M. Shalaby, Synthesis of some novel benzoxazole derivatives as anticancer, anti-HIV-1 and antimicrobial agents, Eur. J. Med. Chem. 40 (9) (2005) 949–959, https://doi.org/10.1016/j.ejmech.2005.03.023.

[15] K. Rurack, M. Spieles, Fluorescence quantum yields of a series of red and near-infrared dyes emitting at 600 − 1000 nm, Anal. Chem. 83 (4) (2011) 1232–1242, https://doi.org/10.1021/ac101329h.

[16] F. Cisnetti, R. Ballardini, A. Credi, M.T. Gandolfi, S. Masiero, F. Negri, S. Pieraccini, G.P. Spada, Photochemical and electronic properties of conjugated bis (azo) compounds: an experimental and computational study, Chem. Eur. J. 10 (8) (2004) 2011–2021, https://doi.org/10.1002/chem.200305590.

[17] A.S. Shawali, Synthesis and tautomerism of aryl- and hetaryl-azo derivatives of bi- and tri-heterocycles, J. Adv. Res. 1 (4) (2010) 255–290, https://doi.org/10.1016/j.jare.2010.07.002.

[18] A.D. Towns, Developments in azo disperse dyes derived from heterocyclic diazo components, Dyes Pigm. 42 (1) (1999) 3–28, https://doi.org/10.1016/S0143-7208(99)00005-4.

[19] A. Lyčka, G.A. Webb, Multinuclear NMR of Azo Dyestuffs, in: Annual Reports on NMR Spectroscopy, Academic Press, 1993, pp. 247–281.

[20] A. Lyčka, 4-Carboxyl-2,6-dinitrophenylazohydroxynaphthalenes tautomerism NMR re-explained, Dyes Pigm. 142 (2017) 51–54, https://doi.org/10.1016/j.dyepig.2017.03.003.

[21] B. Babür, N. Seferoğlu, E. Aktan, T. Hökelek, E. Şahind, Z. Seferoğlu, Phenylazoindole dyes 3: Determination of azo-hydrazone tautomers of new phenylazoindole dyes in solution and solid state, J. Mol. Struct. 1081 (2015) 175–181.

[22] A. Mohammadi, M. Safarnejad, Synthesis, structural characterization and tautomeric properties of some novel bis-azo dyes derived from 5-arylidene-2,4-thiazolidinone, Spectrochim. Acta Part A Mol. Biomol. Spectrosc. 126 (2014) 105–111, https://doi.org/10.1016/j.saa.2014.02.010.

[23] M. Odabaşoğlu, Ç. Albayrak, R. Özkanca, F.Z. Aykan, P. Lonecke, Some polyhydroxy azo–azomethine derivatives of salicylaldehyde: Synthesis, characterization, spectroscopic, molecular structure and antimicrobial activity studies, J. Mol. Struct. 840 (2007) 71–89.

[24] L. Zhang, J.M. Cole, X. Liu, Tuning solvatochromism of azo dyes with intramolecular hydrogen bonding in solution and on titanium dioxide nanoparticles, J. Phys. Chem. C 117 (2013) 26316–26323.

[25] L. Antonín, J. Josef, C. Aleš, ^{15}N, ^{13}C and ^{1}H NMR spectra of the 2:1 cobalt(III) complexes of some azo dyes, Magn. Reson. Chem. 28 (1990) 408–413.

[26] Y. Kurasawa, T. Hosaka, K. Ikeda, Y. Matsumoto, A. Ishikura, A. Takada, H.S. Kim, Y. Okamoto, Substituent effects on the tautomer ratios between the hydrazone imine and diazenyl enamine forms in side-chained quinoxalines, J. Heterocycl. Chem. 31 (1994) 527–533.

[27] A. Lyčka, S. Lunˇák, T. Aysha, R. Holuša, R. Hrdina, A 1H, 13C and 15N NMR spectroscopic and GIAO DFT study of ethyl 5-oxo-2-phenyl-4-(2-

phenylhydrazono)-4,5-dihydro-1H-pyrrole-3-carboxylate, Tetrahedron Lett. 51 (2010) 3149–3151.

[28] J.A. Gutierrez, R.D. Falcone, J.J. Silber, N.M. Correa, Role of the medium on the C343 inter/intramolecular hydrogen bond interactions. An absorption, emission, and 1 HNMR investigation of C343 in benzene/ n -heptane mixtures, J. Phys. Chem. A 114 (27) (2010) 7326–7330, https://doi.org/10.1021/jp102136e.

[29] M. Sigalov, B. Shainyan, N. Chipanina, I. Ushakov, A. Shulunova, Intra- and intermolecular NH···O hydrogen bonds in pyrrolyl derivatives of indane-1,3-dione – experimental and theoretical study, J. Phys. Org. Chem. 22 (2009) 1178–1187.

[30] D.L. Pavia, G.M. Lampman, G.S. Kriz, Introduction to Spectroscopy: A Guide for Students of Organic Chemistry, Harcourt College Publishers, 2001.

[31] A.C. Brown, J. Gibson, XXX.-A rule for determining whether a given benzene mono-derivative shall give a meta-di-derivative or a mixture of ortho- and para-di-derivatives, J. Chem. Soc. Trans. 61 (1892) 367–369.

[32] N. Goutev, H. Matsuura, Hydrogen bonding in chloroform solutions of ethylenedioxy ethers. Spectroscopic evidence of bifurcated hydrogen bonds, J. Phys. Chem. A 105 (2001) 4741–4748.

[33] M.M.M. Raposo, M.C.L.R. Castro, M. Belsley, A.M.C. Fonseca, Push-pull bithiophene azo-chromophores bearing thiazole and benzothiazole acceptor moieties: Synthesis and evaluation of their redox and nonlinear optical properties, Dyes Pigments 91 (2011) 454–465.

[34] M.R. Yazdanbakhsh, A. Mohammadi, M. Abbasnia, Some heterocyclic azo dyes derived from thiazolyl derivatives; synthesis; substituent effects and solvatochromic studies, Spectrochim. Acta Part A Mol. Biomol. Spectrosc. 77 (5) (2010) 1084–1087, https://doi.org/10.1016/j.saa.2010.08.079.

[35] M.A. Satam, R.K. Raut, R.D. Telore, N. Sekar, Fluorescent acid azo dyes from 3-(1,3-benzothiazol-2-yl)naphthalen-2-ol and comparison with 2-naphthol analogs, Dyes Pigm. 97 (2013) 32–42.

[36] A.A. Shabana, I.S. Butler, D.F.R. Gilson, B.J. Jean-Claude, Z.S. Mouhri, M.M. Mostafa, S.I. Mostafa, Synthesis, characterization, anticancer activity and DNA interaction studies of new 2-aminobenzothiazole complexes; crystal structure and DFT calculations of [Ag(Habt)2]ClO4, Inorg. Chim. Acta 423 (2014) 242–255.

[37] M.S. Zakerhamidi, K. Nejati, S. Alidousti, M. Saati, The interactional behaviors and photo-physical properties of azo-salicylaldehyde ligands in solvents media,

Spectrochim. Acta Part A Mol. Biomol. Spectrosc. 150 (2015) 696–703, https://doi.org/10.1016/j.saa.2015.06.015.

[38] G.L. Eakins, J.S. Alford, B.J. Tiegs, B.E. Breyfogle, C.J. Stearman, Tuning HOMO–LUMO levels: trends leading to the design of 9-fluorenone scaffolds with predictable electronic and optoelectronic properties, J. Phys. Org. Chem. 24 (2011) 1119–1128.

[39] F.L. Coelho, C.D.Á. Braga, G.M. Zanotto, E.S. Gil, L.F. Campo, P.F.B. Gonçalves, F.S. Rodembusch, F.D.S. Santos, Low pH optical sensor based on benzothiazole azo dyes, Sensors Actuat. B Chem. 259 (2018) 514–525.

[40] B. Babür, N. Ertan, Part 1: Synthesis and visible absorption spectra of some new monoazo dyes derived from ethyl 2-amino-4-(4′-substitutedphenyl)thiophenes, Spectrochim. Acta Part A Mol. Biomol. Spectrosc. 131 (2014) 319–328.

[41] Hem Joshi, Fadhil S. Kamounah, Cees Gooijer, Gert van der Zwan, Liudmil Antonov, Excited state intramolecular proton transfer in some tautomeric azo dyes and schiff bases containing an intramolecular hydrogen bond, J. Photochem. Photobiol., A 152 (1-3) (2002) 183–191, https://doi.org/10.1016/S1010-6030(02)00155-7.

[42] J.R. Lakowicz, C.D. Geddes, Topics in Fluorescence Spectroscopy: Volume 4: Probe Design and Chemical Sensing, Springer US, 1994.

[43] Xian-Fu Zhang, The effect of phenyl substitution on the fluorescence characteristics of fluorescein derivatives via intramolecular photoinduced electron transfer, Photochem. Photobiol. Sci. 9 (9) (2010) 1261, https://doi.org/10.1039/c0pp00184h.

[44] A.Z. El-Sonbati, A.A. El-Bindary, G.G. Mohamed, Sh.M. Morgan, W.M.I. Hassan, A.K. Elkholy, Geometrical structures, thermal properties and antimicrobial activity studies of azodye complexes, J. Mol. Liq. 218 (2016) 16–34, https://doi.org/10.1016/j.molliq.2016.02.026.

[45] M.E.M. Zayed, R.M. El-Shishtawy, S.A. Elroby, K.O. Al-Footy, Z.M. Al-amshany, Experimental and theoretical study of donor-π-acceptor compounds based on malononitrile, Chem. Central J. 12 (2018) 26.

[46] Tao Tao, Feng Xu, Xiao-Chun Chen, Qian-Qian Liu, Wei Huang, Xiao-Zeng You, Comparisons between azo dyes and Schiff bases having the same benzothiazole/phenol skeleton: Syntheses, crystal structures and spectroscopic properties, Dyes Pigm. 92 (3) (2012) 916–922, https://doi.org/10.1016/j.dyepig.2011.09.008.